coatings

MDPI

Article

Preparation and Isothermal Oxidation Behavior of Zr-Doped, Pt-Modified Aluminide Coating Prepared by a Hybrid Process

Qixiang Fan [1,*], Haojun Yu [2,*], Tie-Gang Wang [1], Zhenghuan Wu [1] and Yanmei Liu [1]

[1] Tianjin Key Laboratory of High Speed Cutting and Precision Machining, Tianjin University of Technology and Education, Tianjin 300222, China; tgwang@tute.edu.cn (T.-G.W.); wzh46817@163.com (Z.W.); ymliu@tute.edu.cn (Y.L.)

[2] Institute of Metal Research, Chinese Academy of Sciences, Shenyang 110016, China

* Correspondence: qxfan2015@163.com (Q.F.); hjyu11s@imr.ac.cn (H.Y.); Tel.: +86-22-8818-1083 (Q.F.); +86-24-8397-8032 (H.Y.)

Academic Editor: Filippo Berto

Received: 16 November 2017; Accepted: 18 December 2017; Published: 21 December 2017

Abstract: To take advantage of the synergistic effects of Pt and Zr, a kind of Zr-doped, Pt-modified aluminide coating has been prepared by a hybrid process, first electroplating a Pt layer and then co-depositing Zr and Al elements by an above-the-pack process. The microstructure and isothermal oxidation behavior of the coating has been studied, using a Pt-modified aluminide coating as a reference. Results showed that the Zr-doped, Pt-modified aluminide coating was primarily composed of β-(Ni,Pt)Al phase, with small amounts of $PtAl_2$- and Zr-rich phases dispersed in it. The addition of Zr diminished voids on the coating surface since Zr could hinder the growth of β-NiAl grains. It also helped to increase the spalling resistance of the oxide scale and reduce the oxidation rate, which made the Zr-doped, Pt-modified aluminide coating possess better oxidation resistance than the reference Pt-modified aluminide coating at the temperature of 1100 °C.

Keywords: Pt-modified aluminide coating; zirconium; oxidation resistance; microstructure; hybrid process

1. Introduction

Aluminide coatings have been used in turbine engines to improve the oxidation resistance and corrosion resistance since they was first developed by General Electric Research Laboratory in 1911. They can be divided into the simple aluminide coating and modified aluminide coatings. The simple aluminide coating is composed of a singular NiAl phase, which can form a continuous and dense layer of Al_2O_3 scale on a surface at high temperatures to protect the components from oxidation and corrosion. The simple aluminide coating possesses good oxidation resistance, but it is susceptible to brittle cracking and sensitive to corrosive elements like sulfur. Thus, various kinds of modified aluminide coatings have been researched to enhance the oxidation resistance and corrosion resistance of the simple aluminide coatings. Beneficial elements like Pt, Cr, Si, and Co, as well as reactive elements are usually added into the simple aluminide coating separately or in combination to form modified aluminide coatings, and results show that these modified aluminide coatings possess better comprehensive properties than the simple aluminide coating [1–4].

Pt-modified aluminide coating has been widely used in turbine engines directly or as a bonding layer for thermal barrier coatings because it possesses much better oxidation resistance and corrosion resistance than the simple aluminide coating [5]. However, there are still voids formed at the metal/oxide interface at high temperature, which accelerate the degradation of the coating [6]. It is

reported that the addition of reactive elements could hinder the outward diffusion of the elements in the alloy and enhance the adhesive strength between the alumina layer and coating by decreasing the formation of voids as well as Kirkendall holes at the metal/oxide interface. To take advantage of the reactive elements, Hf and Dy, etc. have been added to the Pt-modified aluminide coating by many researchers to further increase the service life of the coating [7,8].

As one of the reactive elements, Zr applied to the simple aluminide coating has been studied by many researchers [9–12], and it is proved to be beneficial for enhancing the oxidation resistance since Zr ions can segregate at the grain boundaries of Al_2O_3, preventing the formation of voids at the metal/oxide interface and increasing the adhesion of alumina oxide to the coating. It is also reported by some researchers that Zr can accelerate the formation of α-Al_2O_3 and inhibit the outward diffusion of Al, resulting in a lower oxidation rate [11,13]. In addition, Sitek et al. [14] found that zirconium added to β-NiAl increased its plasticity and corrosion resistance. Moreover, the presence of Zr in the alumina layer aided in lowering the internal stress and increasing the creep resistance [6,15]. Because of these benefits of Zr in the aluminide coating, Hong et al. [16] prepared a Zr-doped, Pt-modified aluminide coating by depositing a layer of Zr using electron beam-physical vapor deposition (EB-PVD) above the Pt-modified aluminide coating, and found that the Pt/Zr co-modified aluminide coating possessed better cyclic oxidation resistance than the Pt-modified aluminide coating, as the Zr-rich oxide pegs formed at the oxide/coating interface increased the resistance to TGO (Thermal Growth Oxide) buckling.

However, the study of the addition of Zr to Pt-modified aluminide coatings is still limited, and there is no report about the microstructure and oxidation behavior of the Zr-doped, Pt-modified aluminide coating prepared by depositing Al and Zr simultaneously on Pt-modified Ni-based superalloys using the above-the-pack process. As we know, the deposition method has an influence on the microstructure and properties of coatings. Thus, to investigate the effect of the Zr element on the oxidation resistance of Pt-modified aluminide coating, a kind of Zr-doped, Pt-modified aluminide coating was prepared by a hybrid process, first electroplating a Pt layer and then depositing Zr and Al elements simultaneously using the above-the-pack process. The microstructure and phase evolution of the Zr-doped, Pt-modified aluminide coating before and after oxidation were been studied in this paper.

2. Materials and Methods

A single crystalline Ni-based superalloy (7.5 wt % Co, 7.0 wt % Cr, 1.5 wt % Mo, 5.0 wt % W, 6.2 wt % Al, 6.5 wt % Ta, 3.0 wt % Re, 0.15 wt % Hf, balanced Ni) was used as the substrate. Specimens with a radius of 15 mm were ground down using 800 # SiC paper, and then sandblasted by alumina balls to increase the surface roughness. After being ultrasonically cleaned within acetone, ethanol, and deionized water, a Pt layer of about 2–4 μm was electroplated on the substrate using a Q5 plating bath (Chemical Process Development, Royston, UK) provided by Skinner [17]. It was operated under the following conditions pH 10.5, current density 5 mA/cm^2, and temperature 92 °C. Then, the specimens were vacuum-annealed at 1080 °C for 2 h to dilute the Pt concentration on the surface. Ultimately, the specimens were hung over a powder mixture composed of FeAl, zirconium tetrachloride, inert filler Al_2O_3, and activator NH_4F in a heating furnace to form Zr-doped, Pt-modified aluminide coating (abbreviated as PtZrAl coating in this paper). For comparison, the Pt-modified aluminide coating (abbreviated as PtAl coating) was also prepared using the power mixture without zirconium tetrachloride in the furnace. The furnace chamber was pumped to at least 10 Pa. Then it was heated to 1080 °C, held for 4 h, and cooled down to room temperature for each preparation process. During the deposition process, a continuous argon flow of about six times furnace volume per hour was provided to avoid the oxidation of the superalloy and the chamber pressure kept at 1 atmosphere.

Isothermal oxidation tests of the PtAl and PtZrAl coatings were conducted in static air at 1100 °C for 320 h. Specimens were placed in alumina crucibles. The crucibles were dried at 1200 °C for 24 h to eliminate the interior volatile impurities as well as gas, and reached constant weights beforehand.

To measure the mass gain of the coatings and obtain the mass gain vs. oxidation time curves, the crucibles were taken out of the furnace and cooled down to room temperature at various intervals. Mass gains of the specimens together with crucibles were measured to count in the mass of the spalled oxide. The sensitivity of the electronic balance was 10^{-4} g. For each test, three parallel samples were applied to acquire the average value of the mass gain, and at least five measurements were taken for each sample.

A D/MAX-RA X-ray diffractometer (XRD, X' Pert PRD, PANalytical, Almelo, The Netherlands) was used for the major phase identification of the coatings before and after oxidation tests. Microstructure and elemental compositions of oxidation products were characterized by a scanning electronic microscope (SEM, Inspect F, Thermo Fisher Scientific, Waltham, MA, USA) equipped with an energy disperse spectroscope (EDS). A layer of Ni-P was electro-plated on the surface of the coatings after oxidation to keep the oxidation scale from being destroyed during the cross-sectional sample preparation process. The electroless plating bath was composed of 20 g/L nickel sulphate, 10 g/L sodium citrate, 30 g/L ammonium chloride, and 30 g/L sodium hypophosphite. Image J software (2.x) was used to calculate the area fraction of γ-Ni/γ'-Ni_3Al phase transited from β-NiAl phase in the outer layer. The detailed procedure was described elaborately in another paper [18]. The thickness of the coatings and alumina scales formed after oxidation was also measured by Image J software (2.x).

3. Results and Discussion

3.1. The Microstructure of the Pt Coating

Figure 1 presents the cross-sectional morphologies of the electroplated Pt coating before and after heat treatment at 1080 °C. The average thickness of the electroplated Pt coating is about 3.2 μm. After heat treatment, the thickness of the coating increases to about 8.6 μm due to the mutual diffusion between the Pt coating and substrate. Driven by the chemical composition gradient, the Pt atoms would migrate into the substrate and elements like Ni, Co, Al, etc. in the substrate would diffuse outward into the Pt coating at the high temperature. There are some discontinuous small black particles in the diffusion coating, which is the alumina left on the original substrate surface due to the sandblasting process.

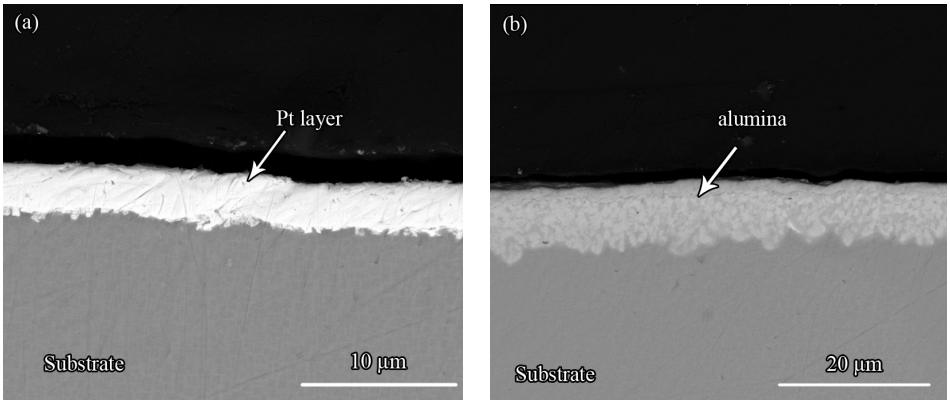

Figure 1. The cross-sectional morphologies of the electroplated Pt coating: (**a**) before treatment at 1080 °C for 2 h; (**b**) after heat treatment at 1080 °C for 2 h.

To figure out the primary phase of the Pt coating after heat treatment, the X-ray diffractometer method was applied to obtain the XRD pattern of the coating, as shown in Figure 2. The main phases post Pt coating are γ-(Ni,Pt) and γ'-$(Ni,Pt)_3Al$. It is reported that the Pt atom possesses high solubility in both of the γ-Ni and γ'-Ni_3Al phases [19–21]. The diffraction peaks of the γ-(Ni,Pt) and γ'-$(Ni,Pt)_3Al$ phases shift to lower angles, compared with the diffraction peaks of the γ-Ni (PDF#04-0850) and γ'-Ni_3Al (PDF#09-0097) phases, since the atomic radius of the Pt atom (0.183 nm) is larger than that of the Ni atom (0.162 nm) [22].

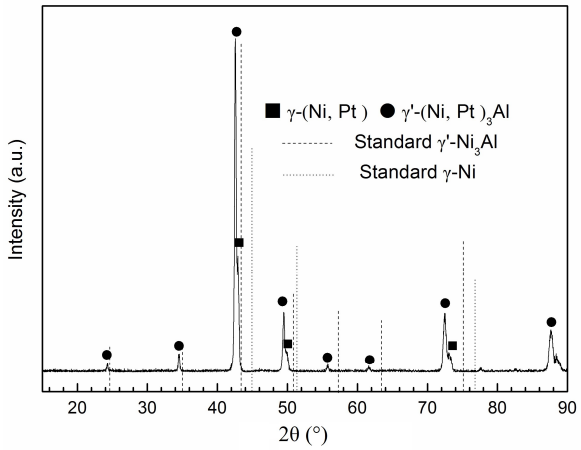

Figure 2. XRD pattern of the electroplated Pt coating after heat treatment at 1080 °C for 2 h.

3.2. The Microstructure of the Zr-Doped, Pt-Modified Aluminide Coating

The XRD patterns of the PtAl and PtZrAl coatings are presented in Figure 3. For the PtAl coating, β-(Ni,Pt)Al phase is the primary phase. The diffraction peaks of the β-(Ni,Pt)Al phase shift to lower angles, compared with those of the β-NiAl phase (PDF#44-1188). This is because the Pt atoms substitute for the Ni sites in the NiAl lattice and the Pt atom possesses larger atomic radius than the Ni atom, which would induce strains as well as stresses resulting in the enlargement of the lattice parameters [23]. In addition, there is a weak diffraction peak at the angle of about 26.05° corresponding to the ξ-$PtAl_2$ phase (PDF#03-1006). Note that the diffraction peak of the $PtAl_2$ phase shifts a little to the higher angle, which is due to the incorporation of the Ni atom in the $PtAl_2$ unit cell. The content of the $PtAl_2$ phase in the Pt-modified aluminide coating is greatly dependent upon the composition of the pack cementation mixture, initial electroplated Pt thickness, and appropriate heat treatment [19,24,25]. Usually a Pt-modified aluminide coating would possess three types of microstructure under different deposition parameters; firstly, the coating of a single β-(Ni,Pt)Al phase, secondly, the coating with binary phases of $PtAl_2$ and β-(Ni,Pt)Al, and thirdly, the coating with a continuous $PtAl_2$ layer formed above the β-(Ni,Pt)Al phase. The Pt-modified aluminide coating prepared in this paper is the second type, and the content of the $PtAl_2$ phase in the PtAl coating is very low. This is because the electroplated Pt layer was annealed before aluminization, leading to a lower Pt content on the surface, and this is beneficial for diminishing or eliminating the $PtAl_2$ phase in the coating.

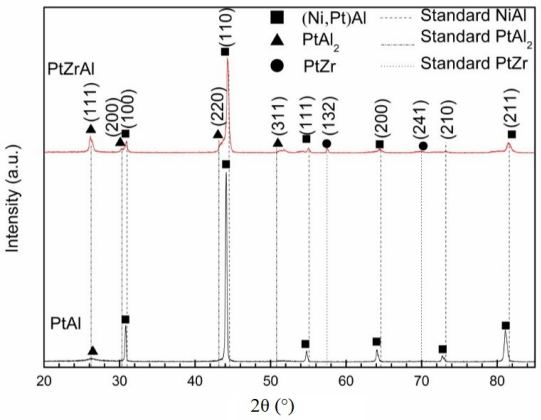

Figure 3. XRD patterns of the Pt coating after aluminization.

When Zr is added to the PtAl coating, the main phase of the coating is still the β-(Ni,Pt)Al phase, and the relative diffraction peaks of the $PtAl_2$ phase become higher. In addition, two minor diffraction

peaks at the angles of about 57.4° and 69.6° correspond to the PtZr phase (PDF#19-0920). It is worthy of note that the diffraction peaks of the β-(Ni,Pt)Al phase shift toward to larger angles, compared with those of the PtAl coating, which might be because more precipitates of Pt forms in the PtZrAl coating and less Pt atoms are dissolved in the β-NiAl phase.

Figure 4 shows the surface morphologies of the PtAl and PtZrAl coatings. For the PtAl coating, the surface is alternated with smooth and irregular rugged microstructures. EDS results show that the predominating elements in both of these two areas are Ni and Al, indicating that the two areas are both composed of β-(Ni,Pt)Al phase, and the black dots in the irregular uneven region are voids formed during the aluminizing process. When the Zr element is added to the PtAl coating, the surface is denser, since Zr tends to segregate around the grain boundaries and hinder the growth of β-NiAl grains. This leads to the formation of smaller particles [13], which is beneficial to diminish the formation of voids on the surface. Note that the PtZrAl coating seems to be etched on the surface, which might be because the zirconium tetrachloride used to deposit Zr was very corrosive. There is some bright precipitated phase around the particle boundaries. The line scanning image of the precipitated phase in larger magnification is presented in Figure 5, and it can be seen that the precipitated phase contains a much higher Zr content than its surrounding areas, which indicates that the bright phase might be a Zr-rich phase.

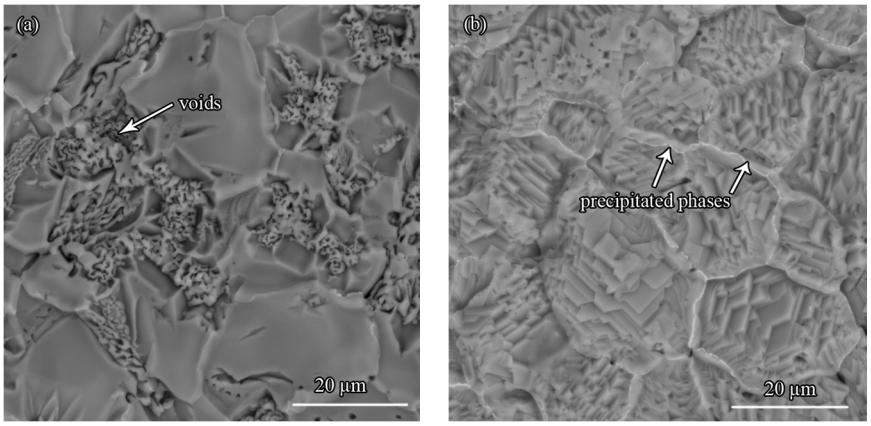

Figure 4. The surface morphologies of the coatings after aluminization: (**a**) PtAl; (**b**) PtZrAl.

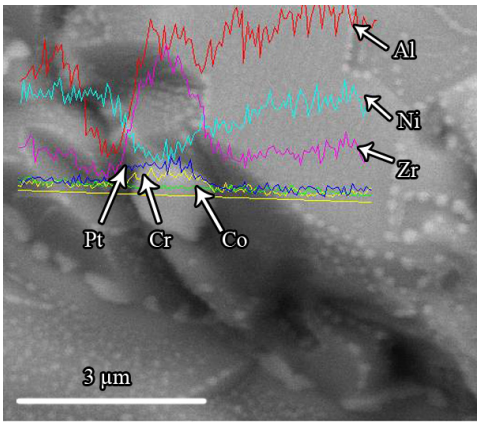

Figure 5. The line scanning image of precipitated phase formed on the surface of the PtZrAl coating.

The cross-sectional morphologies of the PtAl and PtZrAl coatings are presented in Figure 6. As can be seen in Figure 6, both of the two coatings bear a two-layer structure. The outer layer of the PtAl coating is mainly the β-(Ni,Pt)Al phase, and the $PtAl_2$ phase is nearly invisible since the diffraction peaks of the $PtAl_2$ phase is very low, as shown in Figure 3. In the inner layer, there are

some bright white precipitated phases rich in Cr, W, Ta, etc., which form due to the mutual diffusion between the substrate and coating. At the temperature of 1080 °C, the Ni atoms possess high activity and the coating forms primarily through the singular outward diffusion of Ni atoms. The depletion of Ni atoms in the substrate near the original surface would lead to the transition of the γ-Ni phase into the β-NiAl phase. Since the solubility of Cr, W, Ta, etc. in the γ phase is higher than that in the β phase, the phases rich in refractory elements precipitate from the β phase. The average chemical compositions of the PtAl coating in the outer layer are 49.0Al-1.6Cr-4.0Co-41.2Ni-4.3Pt (at.%). According to the cross-sectional morphologies, the thicknesses of the PtAl coating is about 53 ± 1 μm.

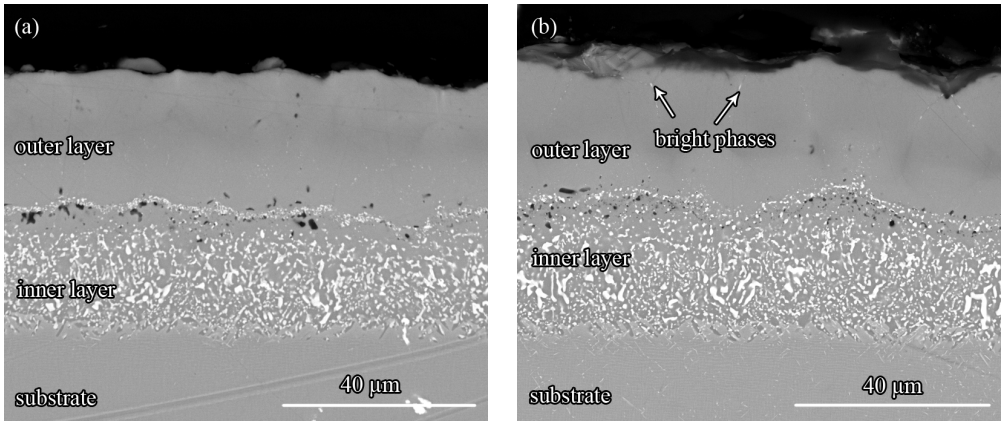

Figure 6. The cross-sectional morphologies of the coatings after aluminization: (**a**) PtAl; (**b**) PtZrAl.

As for the PtZrAl coating, the cross-sectional morphology is nearly similar to the PtAl coating, but some bright phases could be distinctly observed in the outer layer. The average compositions of the PtZrAl coatings in the outer layer are 48.3Al-1.6Cr-3.8Co-41.9Ni-3.9Pt-0.5Zr (at.%), detected by EDS, and the compositions of the bright phases are 42.6Al-3.7Cr-4.8Co-42.0Ni-4.1Pt-2.8Zr (at.%), revealing that the bright phases contain higher Zr contents than the surrounding β phase. The solubility of the Zr element in the NiAl phase is still unknown, but the diameter of the zirconium atom is much larger than the interplanar spacings of the β-NiAl phase, so it is hard to dissolve much Zr in the NiAl phase. It is estimated that 0.2–0.4 at.% Zr could be dissolved in the aluminide coating [6]. Some research showed that Zr tended to segregate around the NiAl grain boundary as Zr particles or combine with other elements in the form of compounds like Ni_7Zr_2, NiAl-Zr, or Al_5Ni_2Zr, etc. [12,16,26,27]. Combined with the XRD diffraction pattern shown in Figure 3 and the line scanning image (Figure 5), it can be inferred that the Zr element might be partly saturated in the β-NiAl phase and partly co-segregated with Pt around the grain boundary of the β-NiAl phase. However, to figure out why Zr co-segregated with Pt and the accurate sites of the Zr-rich phases, other techniques such as TEM are needed, which we will perform in future study. The whole thickness of the PtZrAl coating is about 55 ± 1 μm, which is slightly thicker than the PtAl coating.

3.3. Oxidation Kinetic Curve

Figure 7 presents the mass gain versus time of the PtAl and PtZrAl coatings after isothermal oxidation at 1100 °C for 320 h. The mass change curves of these two coatings conform to the same law. During the initial 50 h, the mass gains increase greatly since the coatings are oxidized quickly when they are exposed to the high temperature. Then the mass gains continue steadily, for protective and dense oxide layers could be formed on the surface after the initial oxidation, which can protect the coatings from further oxidation. The mass gain of the PtZrAl coating is a little higher than that of the PtAl coating in the first 10 h. After that, the PtZrAl coating possesses lower mass gain than the PtAl coating. The maximum mass gain of the PtAl and PtZrAl coatings is about 1.30 and 1.17 mg/cm^2,

respectively. It can be inferred that the addition of Zr would decrease the oxidation rate of the Pt-modified aluminide coating and increase the oxidation resistance.

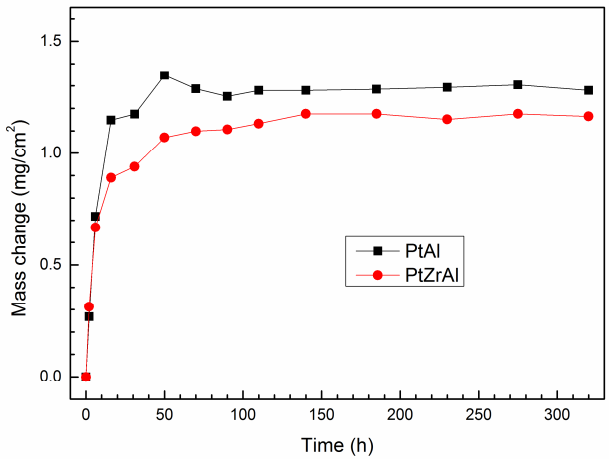

Figure 7. The mass gain versus time of the PtAl and PtZrAl coatings after isothermal oxidation at 1100 °C.

3.4. Oxidation Product

The XRD patterns of the PtAl and PtZrAl coatings after isothermal oxidation at 1100 °C for 2 h and 320 h are presented in Figure 8. It can be seen that the main phase of the PtAl and PtZrAl coatings is still β-NiAl, and the diffraction peaks of α-Al_2O_3 emerge in the two coatings after oxidation for 2 h. The $PtAl_2$ phase is not detected, which might be because the $PtAl_2$ phase transforms into β-PtAl, and then changes to β-NiAl during the oxidation process [16]. As the oxidation time proceeds to 320 h, the diffraction peaks of the α-Al_2O_3 become much stronger and the main phase of the two coatings transits to the γ'-Ni_3Al phase, although the β-NiAl phase could still be detected.

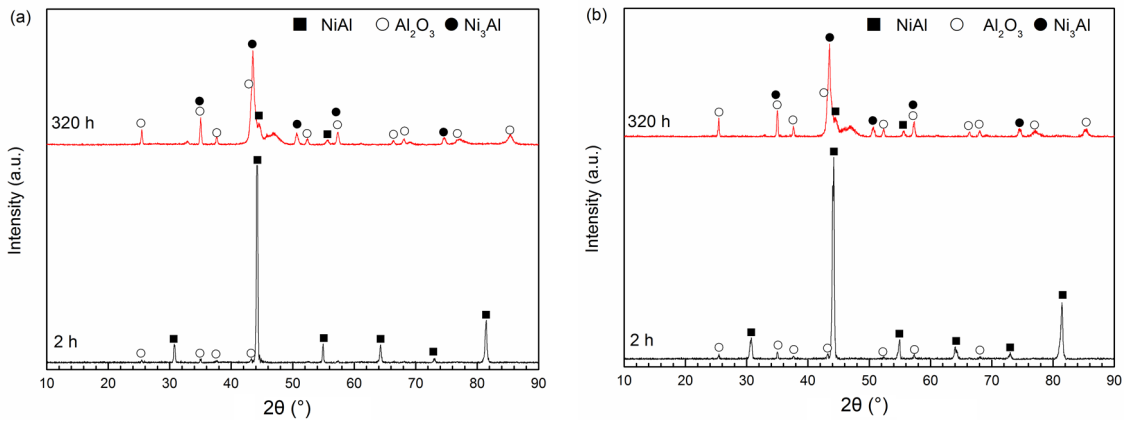

Figure 8. XRD patterns of the coatings after isothermal oxidation at 1100 °C for 2 h and 320 h: (**a**) PtAl; (**b**) PtZrAl.

Figure 9 shows the cross-sectional morphologies of the PtAl and PtZrAl coatings after oxidation for 2 h. It can be seen that a very thin alumina layer was formed on the surface of the PtAl and PtZrAl coatings. According to Wagner's theory, if the less noble metal can diffuse with a sufficient rate towards the coating/oxide interface, then the exclusive oxidation of this element can be attained. Since the Gibbs free energy of Al_2O_3 is much smaller than that of oxides like NiO, Cr_2O_3, etc., and the Al content in the coatings is up to 50 at.%, which is much higher than the minimum Al content needed to sustain its exclusive oxidation, then a dense and continuous Al_2O_3 layer is formed on the surface [28].

Since the oxidation time is limited, the thickness of the Al_2O_3 layer is very small, and this is the reason why the diffraction peaks of the alumina are very weak after oxidation for 2 h, as presented in Figure 8.

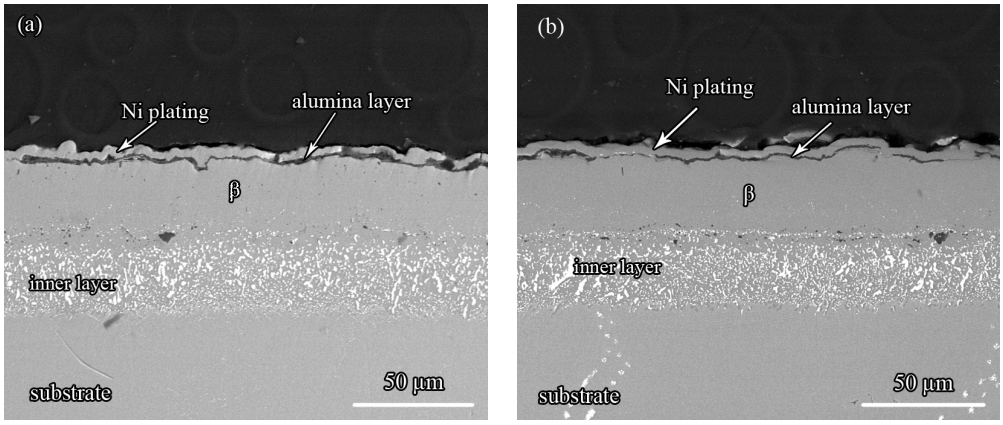

Figure 9. The cross-sectional morphologies of the coatings after oxidation at 1100 °C for 2 h: (**a**) PtAl; (**b**) PtZrAl.

Figure 10 presents the surface morphologies of the PtAl and PtZrAl coatings after oxidation at 1100 °C for 320 h. As can be seen in Figure 10a, the surface of the PtAl coating is mainly composed of alumina with some white phase dispersed in it. The chemical compositions of the alumina (area A in Figure 10a) and the white phase (area B in Figure 10a) on the surface are shown in Table 1. The white phase contains high Ni content (48.7 at.%) and small amounts of other alloying elements such as Co, Cr, W, and Pt, indicating that the elements in the coating diffuse outward. The presence of the white phase also might be due to the spallation of the alumina layer, which results in the exposure of the coating underneath. Severe spallation occurs on the surface of the PtAl coating, as shown in Figure 10a. For the PtZrAl coating, there are also some white phases that emerged on the surface, but their quantity and size are less and smaller than those in the PtAl coating. Like the white phases on the surface of the PtAl coating, these white phases also contain a high Ni content as well as other alloying elements. Compared with the PtAl coating, the alumina layer on the PtZrAl coating is dense and continuous in the image with low magnification, and no visible spallation nor crack occurs on the surface. Only in the larger magnification image can some cracks be observed. This reveals that the addition of Zr improves the spalling resistance of the alumina scale.

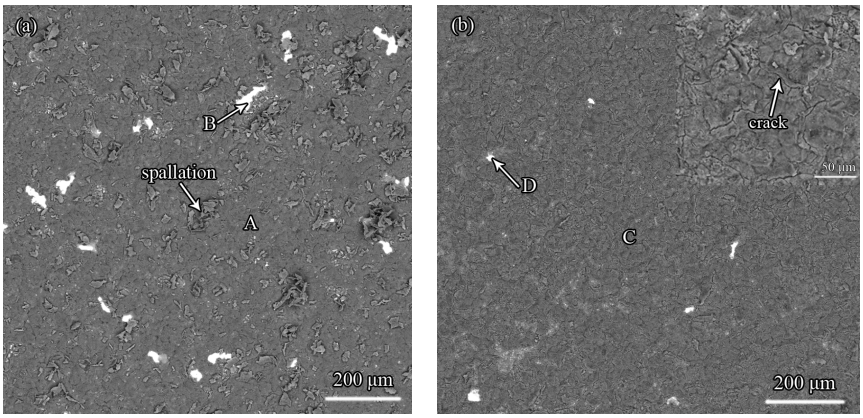

Figure 10. The surface morphologies of the coatings after oxidation at 1100 °C for 320 h: (**a**) PtAl and (**b**) PtZrAl.

Table 1. Elemental compositions of four different spots (A, B, C, D) on the surface images (Figure 10) of the PtAl and PtZrAl coatings after oxidation for 320 h.

Spot	Al (at.%)	O (at.%)	Ni (at.%)	W (at.%)	Cr (at.%)	Co (at.%)	Pt (at.%)	Hf (at.%)
A	46.4	50.2	1.6	1.9	–	–	–	–
B	18.2	19.3	48.7	3.0	3.0	5.3	2.4	0.2
C	37.3	59.3	1.0	2.4	–	–	–	–
D	13.8	30.6	41.8	4.8	2.4	4.7	2.0	–

The cross-sectional morphologies of the PtAl and PtZrAl coatings after oxidation at 1100 °C for 320 h are shown in Figure 11. In Figure 11, a layer of alumina is formed on the surface of both coatings. Compared with the oxidation scale shown in Figure 9, the thickness of the oxidation layer becomes thicker, revealing that the alumina layer grows slowly with the oxidation. When a dense oxide layer is formed on the surface, the diffusion rates of oxygen and nitrogen are decreased dramatically, but there is still a small quantity of oxygen that could migrate into the coating and react with the Al element. This process leads to the constant consumption of the beneficial element Al and phase transition from β to γ'. The thickness of the alumina layer on the surface of the PtAl and PtZrAl coatings is about 5 ± 1 μm and 4 ± 1 μm, respectively. The light grey area beneath the alumina scale is γ'-Ni_3Al, while the dark grey phase is β-NiAl. The area fractions of the γ'-Ni_3Al phase in the outer layer of the two coatings are about 10.1% and 6.9%, respectively, indicating that more beneficial β-NiAl phase is consumed in the PtAl coating than that in the PtZrAl coating. Besides the outward diffusion to sustain the exclusive growth of the Al_2O_3 layer, the Al element also diffuses into the substrate under the chemical composition gradient, which makes the β phase transform into γ' phase in the inner layer. When the Al element is completely consumed, the coating will fail to protect the substrate from oxidation. Note that the particle size of the bright precipitated phases rich in refractory elements in the inner layer becomes larger while the number decreases, compared with the microstructure (Figure 6) before oxidation. This is because, on one hand, the precipitated phases will grow up by absorbing other refractory elements nearby, and on the other hand, they will dissolve gradually when the surrounding β phase has transformed into γ' phase due to the higher solubility of refractory elements in the γ' phase. In summary, although certain amounts of Al are consumed, there is still a large amount of β phase left in both the PtAl and PtZrAl coatings, indicating that these two coatings possess good oxidation resistance and could still keep the substrate from further oxidation, even after oxidation for 320 h. However, the alumina layer formed on the PtZrAl coating is thinner than that formed on the PtAl coating and less β phase is consumed in the PtZrAl coating, demonstrating that the PtZrAl coating is oxidized more mildly than the PtAl coating and possesses better oxidation resistance.

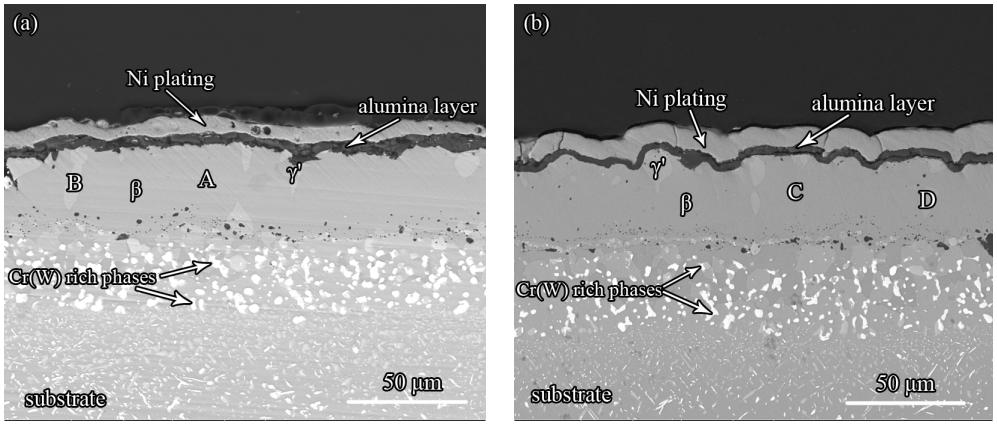

Figure 11. The cross-sectional morphologies of the coatings after oxidation at 1100 °C for 320 h: (**a**) PtAl; (**b**) PtZrAl.

3.5. The Effect of Zr on the Oxidation Resistance of the Pt-Modified Aluminide Coating

When the coatings are exposed to the high temperature, the transient alumina such as γ, δ, and θ would be formed first, after which they transform into the stable α-Al_2O_3 phase with the process of oxidation. It is reported that the transient alumina grows primarily by the outward diffusion of Al, while the stable α-Al_2O_3 phase forms mainly by the inward diffusion of O [29]. Some researchers revealed that Zr tends to segregate at the metal-scale interface and scale grain boundary [10,30], and could act as ionic clusters to constrain the outward transport of Al ions by physical obstruction as well as chemical interaction on the cation diffusion pathways [13,31]. This effect of suppressing the outward diffusion of Al ions is beneficial for reducing the formation of transient alumina and promoting the formation of stable alumina. Zhou et al. revealed that Zr could provide nucleation sites for the growth of α-Al_2O_3 and accelerate the θ-Al_2O_3 to α-Al_2O_3 phase transformation [26]. The growth rate of the transient alumina is higher than that of α-Al_2O_3 [11]; thus, the quick formation of α-Al_2O_3 is in favor of lowering the oxidation rate. In addition, the voids formed on the surface of the PtAl coating could provide a diffusion path to the inward diffusion of O and increase the oxidation rate. Consequently, the Zr-doped, Pt-modified aluminide coating possesses a lower oxidation rate than the Pt-modified aluminide coating.

The rumpling and spalling resistance is critical to the properties of a coating. The mechanism of rumpling is still unknown, but it is accepted that internal stress in the oxide scale is a main factor leading to rumpling [18]. Usually, internal stress primarily originates from two aspects: growth stress developed isothermally during oxide formation and thermal stress generated during thermal cycling due to the thermal expansion mismatch between the oxide and alloy [10]. Some researchers found that the β to γ' phase transformation in the outer layer would also induce large compressive stress because of the volume shrinkage up to 38% [32,33]. Since only a bit of Zr is added into the Pt-modified aluminide coating, the thermal expansion coefficient variation of the coating and oxide induced by Zr might be omitted. Thus, the difference between the rumpling resistance of the Pt-modified aluminide coating with or without Zr might be primarily dependent upon to the growth stress and compressive stress caused by the β to γ' phase transformation. It is known that the Pilling-Bedworth Ratio (PBR) of Al is larger than 1, and the PBR of the transient alumina is bigger than that of stable α-Al_2O_3 [34], which means that less compressive stress would be generated in the alumina scale if more α-Al_2O_3 phase was formed during the oxidation process. As mentioned above, the addition of Zr is beneficial for promoting the formation of the α-Al_2O_3 phase, thus the compressive growth stress generated in the Zr-doped, Pt-modified aluminide coating might be smaller than that in the Pt-modified aluminide coating. Also, there is less β phase transformed into γ' phase in the Zr-doped, Pt-modified aluminide coating, which means that less compressive stress would be formed in the coating and scale. In addition, Zr is reported to aid in increasing the creep resistance and lowering the internal stress [6]. When the internal stress in the alumina layer is too high, it will lead to crack and even spallation of the alumina scale. Consequently, the crack and spallation on the surface of the Zr-doped, Pt-modified aluminide coating is milder than that on the Pt-modified aluminide coating. It is confusing that the oxide scales of PtZrAl appear more rumpled than the PtAl coating, which might be because the crack and spallation on the PtAl coating surface would release stress in the alumina scale and decrease the scale deformation.

4. Conclusions

A new type of Zr-doped, Pt-modified aluminide coating has been prepared by a hybrid method, by first electroplating a Pt layer and then depositing Zr and Al elements simultaneously. The main phases of the electroplated Pt layer after vacuum-annealing are γ-(Ni,Pt) and γ'-$(Ni,Pt)_3Al$. After the co-deposition of Al and Zr, the primary phase of the coating becomes the β-(Ni,Pt)Al phase with small amounts of $PtAl_2$- and Zr-rich phases dispersed in it. The average content of Zr in the coating is about 0.5 at.%, and it plays a role in decreasing the voids on the surface of the Pt-modified aluminide coating.

The isothermal oxidation experiment shows that the Zr-doped, Pt-modified aluminide coating possesses lower mass gain and a thinner alumina layer than the Pt-modified aluminide coating. In addition, the crack and spallation on the surface of the Zr-doped, Pt-modified aluminide coating is milder than that on the Pt-modified aluminide coating after oxidation at 1100 °C for 320 h. It can be concluded that the addition of Zr to the Pt-modified aluminide coating could improve the oxidation resistance, since Zr could promote the formation of the stable α-Al_2O_3 phase and decrease the internal stress in the oxide scale.

Acknowledgments: This work was financially supported by the National Nature Science Foundation of China (Grant Nos. 51501130 and 51301181), Research project of Tianjin Municipal Education Commission (Grant No. JWK1711), Tianjin Key Research Program of Application Foundation and Advanced Technology (Grant No. 15JCZDJC39700), and Innovation Team Training Plan of Tianjin Universities and Colleges (Grant No. TD12-5043), The Research Development Foundation of Tianjin University of Technology and Education (KJ11-06).

Author Contributions: Qixiang Fan performed the oxidation experiments and analyzed the data; Haojun Yu designed the experiments and prepared the coatings. Tie-Gang Wang, Zhenghuan Wu, and Yanmei Liu contributed to data analysis; Qixiang Fan wrote the paper; all authors participated and discussed this work and contributed to the submitted and published manuscript.

Conflicts of Interest: The authors declare no conflict of interest.

References

1. Song, Y.; Murakami, H.; Zhou, C. Cyclic-oxidation behavior of multilayered Pt/Ru-modified aluminide coating. *J. Mater. Sci. Technol.* **2011**, *27*, 280–288. [CrossRef]
2. Wu, D.; Jiang, S.; Fan, Q.; Gong, J.; Sun, C. Hot corrosion behavior of a Cr-modified aluminide coating on a Ni-based superalloy. *Acta Metall. Sin. (Engl. Lett.)* **2014**, *27*, 627–634. [CrossRef]
3. Fan, Q.X.; Jiang, S.M.; Wu, D.L.; Gong, J.; Sun, C. Microstructure and hot corrosion behaviors of two Co modified aluminide coatings on a Ni-based superalloy at 700 °C. *Appl. Surf. Sci.* **2014**, *311*, 214–223. [CrossRef]
4. Dai, P.; Wu, Q.; Ma, Y.; Li, S.; Gong, S. The effect of silicon on the oxidation behavior of NiAlHf coating system. *Appl. Surf. Sci.* **2013**, *271*, 311–316. [CrossRef]
5. Liu, R.; Jiang, S.; Yu, H.; Sun, C. Preparation and hot corrosion behaviour of Pt modified AlSiY coating on a Ni-based superalloy. *Corros. Sci.* **2016**, *104*, 162–172. [CrossRef]
6. Zagula-Yavorska, M.; Morgiel, J.; Romanowska, J.; Sieniawski, J. Nanoparticles in zirconium-doped aluminide coatings. *Mater. Lett.* **2015**, *139*, 50–54. [CrossRef]
7. Yang, Y.; Jiang, C.; Yao, H.; Bao, Z.; Zhu, S.; Wang, F. Preparation and enhanced oxidation performance of a Hf-doped single-phase Pt-modified aluminide coating. *Corros. Sci.* **2016**, *113*, 17–25. [CrossRef]
8. Zhou, Z.; Peng, H.; Zhang, L.; Guo, H.; Gong, S. Microstructure and cyclic oxidation behaviour of low-Pt/Dy co-doped β-NiAl coatings on single crystal (SC) superalloy. *Surf. Coat. Technol.* **2016**, *304*, 108–116. [CrossRef]
9. Khakpour, I.; Soltani, R.; Sohi, M.H. Microstructure and high temperature oxidation behaviour of Zr-doped aluminide coatings fabricated on nickel-based super alloy. *Procedia Mater. Sci.* **2015**, *11*, 515–521. [CrossRef]
10. Pint, B.A.; Wright, I.G.; Lee, W.Y.; Zhang, Y.; Prüßner, K.; Alexander, K.B. Substrate and bond coat compositions: Factors affecting alumina scale adhesion. *Mater. Sci. Eng. A* **1998**, *245*, 201–211. [CrossRef]
11. Hamadi, S.; Bacos, M.P.; Poulain, M.; Seyeux, A.; Maurice, V.; Marcus, P. Oxidation resistance of a Zr-doped NiAl coating thermochemically deposited on a nickel-based superalloy. *Surf. Coat. Technol.* **2009**, *204*, 756–760. [CrossRef]
12. Zagula-Yavorska, M.; Pytel, M.; Romanowska, J.; Sieniawski, J. The Effect of Zirconium Addition on the Oxidation Resistance of Aluminide Coatings. *J. Mater. Eng. Perform.* **2015**, *24*, 1614–1625. [CrossRef]
13. Wei, L.; Peng, H.; Jia, F.; Zheng, L.; Gong, S.; Guo, H. Cyclic oxidation behavior of Hf/Zr co-doped EB-PVD β-NiAl coatings at 1200 °C. *Surf. Coat. Technol.* **2015**, *276*, 721–725. [CrossRef]
14. Sitek, R.; Kwaśniak, P.; Sopicka-Lizer, M.; Borysiuk, J.; Kamiński, J.; Mizera, J.; Kurzydłowski, K.J. Experimental and ab-initio study of the Zr- and Cr-enriched aluminide layer produced on an IN 713C Inconel substrate by CVD; investigations of the layer morphology, structural stability, mechanical properties, and corrosion resistance. *Intermetallics* **2016**, *74*, 15–24. [CrossRef]
15. Cho, J.; Wang, C.M.; Chan, H.M.; Rickman, J.M.; Harmer, M.P. Role of segregating dopants on the improved creep resistance of aluminum oxide. *Acta Mater.* **1999**, *47*, 4197–4207. [CrossRef]

16. Hong, S.J.; Hwang, G.H.; Han, W.K.; Lee, K.S.; Kang, S.G. Effect of zirconium addition on cyclic oxidation behavior of platinum-modified aluminide coating on nickel-based superalloy. *Intermetallics* **2010**, *18*, 864–870. [CrossRef]
17. Skinner, P.E. Improvements in platinum plating: A new generation of electroplating baths. *Platin. Met. Rev.* **1989**, *33*, 102–105.
18. Liu, R.; Jiang, S.; Guo, C.; Gong, J.; Sun, C. The alumina scale growth and interdiffusion behaviour of Pt modified AlSiY coating during cyclic oxidation. *Corros. Sci.* **2017**, *120*, 121–129. [CrossRef]
19. Wang, Y.Q.; Sayre, G. Factors affecting the microstructure of platinum-modified aluminide coatings during a vapor phase aluminizing process. *Surf. Coat. Technol.* **2009**, *203*, 1264–1272. [CrossRef]
20. Mollard, M.; Pedraza, F.; Bouchaud, B.; Montero, X.; Galetz, M.C.; Schutze, M. Influence of the superalloy substrate in the synthesis of the Pt-modified aluminide bond coat made by slurry. *Surf. Coat. Technol.* **2015**, *270*, 102–108. [CrossRef]
21. Jackson, M.R.; Rairden, J.R. The aluminization of platinum and platinum-coated IN-738. *Metall. Trans. A* **1977**, *8*, 1697–1707. [CrossRef]
22. Hong, S.J.; Hwang, G.H.; Han, W.K.; Kang, S.G. The effect of Pt contents on the surface morphologies of Pt-modified aluminide coating. *Surf. Coat. Technol.* **2009**, *203*, 3066–3071. [CrossRef]
23. Pedraza, F.; Kennedy, A.D.; Kopecek, J.; Moretto, P. Investigation of the microstructure of platinum-modified aluminide coatings. *Surf. Coat. Technol.* **2006**, *200*, 4032–4039. [CrossRef]
24. Krishna, G.R.; Dasa, D.K.; Singhb, V.; Joshia, S.V. Role of Pt content in the microstructural development and oxidation performance of Pt–aluminide coatings produced using a high-activity aluminizing process. *Mater. Sci. Eng. A* **1998**, *251*, 40–47. [CrossRef]
25. Benoist, J.; Badawi, K.F.; Malie, A.; Ramade, C. Microstructure of Pt modified aluminide coatings on Ni-based superalloys without prior Pt diffusion. *Surf. Coat. Technol.* **2005**, *194*, 48–57. [CrossRef]
26. Zhou, Y.; Zhao, X.; Zhao, C.; Hao, W.; Wang, X.; Xiao, P. The oxidation performance for Zr-doped nickel aluminide coating by composite electrodepositing and pack cementation. *Corros. Sci.* **2017**, *123*, 103–115. [CrossRef]
27. Qian, L.; Fang, X.; Voisey, K.T.; Nekouie, V.; Zhou, Z. Incorporation and evolution of ZrO_2 nano-particles in Pt-modified aluminide coating for high temperature applications. *Surf. Coat. Technol.* **2017**, *311*, 238–247. [CrossRef]
28. Fan, Q.X.; Peng, X.; Yu, H.J.; Jiang, S.M.; Gong, J.; Sun, C. The isothermal and cyclic oxidation behaviour of two Co modified aluminide coatings at high temperature. *Corros. Sci.* **2014**, *84*, 42–53. [CrossRef]
29. Prescott, R.; Mitchell, D.F.; Graham, M.J.; Doychak, J. Oxidation mechanisms of β-NiAl + Zr determined by SIMS. *Corros. Sci.* **1995**, *37*, 1341–1364. [CrossRef]
30. Wang, C.M.; Cargill, G.S., III; Harmer, M.P.; Chan, H.M.; Cho, J. Atomic structural environment of grain boundary segregated Y and Zr in creep resistant alumina from EXAFS. *Acta Mater.* **1999**, *47*, 3411–3422. [CrossRef]
31. Guo, H.; Li, D.; Zheng, L.; Gong, S.; Xu, H. Effect of co-doping of two reactive elements on alumina scale growth of β-NiAl at 1200 °C. *Corros. Sci.* **2014**, *88*, 197–208. [CrossRef]
32. Yang, L.; Zou, Z.; Kou, Z.; Chen, Y.; Zhao, G.; Zhao, X.; Guo, F.; Xiao, P. High temperature stress and its influence on surface rumpling in NiCoCrAlY bond coat. *Acta Mater.* **2017**, *139*, 122–137. [CrossRef]
33. Bouchaud, B.; Balmain, J.; Pedraza, F. Cyclic and isothermal oxidation at 1100 °C of a CVD aluminised directionally solidified Ni superalloy. *Oxid. Met.* **2008**, *69*, 193–210. [CrossRef]
34. Ke, P.; Wang, Q.; Hua, W.; Gong, J.; Sun, C.; Zhou, Y. Stresses and microstructural development of thermal barrier coatings using AIP/D-gun two-step processing. *J. Am. Ceram. Soc.* **2007**, *90*, 936–941. [CrossRef]